Very Long-Wavelength $GaAs/Al_xGa_{1-x}As$ Infrared Hot Electron Transistor

S. D. Gunapala, J. S. Park, T. L Lin, and J. K. Liu

Center for Space Microelectronics Technology, Jet Propulsion Laboratory, California Institute of Technology, Pasadena,CA91109

K. M. S. V. Bandara

Department of Physics, University of Peradeniya, Peradeniya, Sri Lanka

ABSTRACT

We have demonstrated a bound to continuum state $GaAs/Al_xGa_{1-x}As$ infrared hot electron transistor which has a peak response at λ_p = 16.3 μm. This device utilizes a bound-to-continuum quantum well infrared photodetector as a photosensitive emitter and a wide $AI_xG\ a_{1-x}As$ barrier between the base and the collector as an energy discriminating filter. An excellent photo-current transfer ratio of α_p = 0..12 and very low dark current transfer ratio of α_{dark}: 7.2x10-5 is achieved at a temperature of T = 60 K.

Infrared (IR) detectors and imaging systems that operate in the wavelength range 3-18 μm are required in many space applications such as monitoring the global atmospheric temperature profiles, relative humidity profiles, cloud characteristics, and the distribution of minor constituents in the atmosphere which are being planned for the NASA's Earth Observing System (EOS). These space applications have placed stringent requirements on the performance of the IR detectors and arrays including high defectivity, low dark current, uniformity, radiation hardness and lower power dissipation. Also this spectral region is rich in information vital to the understanding of composition, structure and the energy balance of molecular clouds and star forming regions of our galaxy. Thus, there is a great interest in IR detectors operating both inside and outside the atmospheric windows (3 -5 μm and 8-12 pm).

Since the GaAs based quantum well infrared photodetectors (QWIPs)[1-13] which utilize the intersubband transitions meet most of the above mentioned requirements, these detectors should be very attractive for the detection of IR radiation in the 6- 18 μm spectral range. However the only problem associated with the very long wavelength QWIPs (k> 12 μm) is the higher dark current which adversely affects detector performance. By analyzing the dark current of shallow quantum wells which were designed for very long wavelength operation, we have realized that at low temperatures (< 60 K) the total tunneling contribution of the dark current (sequential tunneling + therrnionic assisted tunneling) is significantly higher than the thermionic contribution of the dark current (Fig. 1). The conduction electrons carrying these two tunneling current components are lower in energy than the photoelectrons 8 Thus, an IR hot electron transistor (IHET)[14-16], which has an additional wide $Al_xGa_{1-x}As$ barrier to filter out sequential tunneling and therrnionic assisted tunneling currents will perform better at very long wavelength than QWIP.

In order to analyze the dark current of a QWIP which has a intersubband absorption peak at 16 μm, we first calculated the effective number of electrons [11,17] n(V) which are thermally excited into the continuum transport states, as a function of bias voltage V, using the following expression.

$$n(V) = \left(\frac{m^*}{\pi\hbar^2 L_p}\right)\int_{E_0}^{\infty} f(E)T(E,V)dE \qquad (1)$$

The first factor containing the effective mass m* represents the average three dimensional density of states. Where L_p is the superlattice period, f(E) is the Fermi factor $f(E) = [1+\exp(E-E_0-E_F)/KT]^{-1}$, E_0 is the bound state energy, E_F is the two-dimensional Fermi energy, E is the energy of the electron, and T(E,V) is the tunneling current transmission factor which is obtained by using WKB approximation to a biased quantum well. In equation 1, the effective number of electrons above the barrier account for thermionic contribution and the number of electrons below the barrier account for thermionic assisted tunneling and tunneling contribution of the dark current. Then the bias-dependent dark current $I_d(V)$ was calculated, using $I_d(V) = eAn(V)v(V)$, where v(V) is the average transport velocity , A is the device area, and e is the electronic charge. The average transport velocity was calculated using $v(V) = \mu F[1+(\mu F/v_s)^2]^{-1/2}$, where μ is the mobility, F is the electric field, and v_s is the saturated drift velocity. In order to obtain T = 60K, bias-dependent dark current $\mu = 1200\ cm^2/Vs$ and vs = 5.5x106 cm/s was used. Fig. 1 shows the T= 60K dark current due to therm ionic emission, total dark current (thermionic + thermionic assisted tunneling + tunneling), and experimental dark current of a QWIP sample which has wavelength cutoff λ_c = 17.8 p.m. According to the calculations tunneling through the barriers dominate the dark current at temperatures below 30K, at temperatures between 30-55 K thermionic assisted tunneling might become important, and at temperatures above 55 K thermionic emission into the continuum transport states dominate the dark current.

As shown in Fig. 2 the device structure consisted of a multi-quantum well region of 50 periods of 500 Å undoped $Al_{0.11}Ga_{0.89}As$ barrier and 65 Å doped GaAs well. The quantum wells were doped to $n = 5x10^{17}\ cm^{-3}$, and sandwiched between a heavily doped ($n = 1x10^{18}\ cm^{-3}$) 1 μm GaAs contact layer at the bottom as the emitter contact and a doped ($n = 3x10^{17}\ cm^{-3}$) 500 Å GaAs layer on the top as the base contact. On top of the base a 2000 Å undoped $Al_{0.11}Ga_{0.89}As$ layer and a doped ($n = 3x10^{17}\ cm^{-3}$) 0.5 μm GaAs layer were grown. The 2000 Å undoped $Al_{0.11}Ga_{0.89}As$ As layer acted as a discriminator between the tunnel-electrons and photo-electrons, and the top 0.5 μm GaAs layer served as the collector. This device structure was grown on a semi-insulating GaAs substrate using molecular beam epitaxy. The inset of the Fig. 2 shows the diagram of the-device. QWIP operation can be obtained between the emitter and the base and all the terminals (three) are required for the IHET operation. The IHET currents were measured at the collector (low energy tunneled electrons drain through the base).

To facilitate the application of bias to the quantum well structure, the following processing steps *were* carried out. First arrays of *200x200* μm^2 square collectors were chemically etched. In the next processing step the 6.25x 10^{-4} cm^2 QWIP mesas which overlap with collector mesas were etched. Finally, Au/Ge ohmic contacts were evaporated onto the emitter, base and collector contact layers. The emitter and collector dark currents versus base-collector bias voltage are shown in Fig. 3. This figure also shows the excellent dark current filtration capability of the quantum filter. The dark current transfer ratio $\left(\alpha_d = I_{C(dark)} / I_{E(dark)}\right)$ is 7.2x10^{-5} at operating base-collector bias voltage V_{CB} = -42 mV (Fig. 3).

The intersubband absorption was measured on a 45" polished multipass waveguide[2] at T = 60K and absorption coefficient α_p = 694 cm-l at λ_p = 17.1 μm was obtained. This α_p corresponds to an unpolarized absorption quantum efficiency $\eta = (1 - e^{-2\alpha l}) / 2 = 16.5\%$. Also these 200x200 μm^2 square detectors were back illuminated through a 45" polished facet as previously described in detail [1] and responsivity spectrums were measured with a tunable source consisting of a 1000K blackbody and a grating monochromator. The emitter and collector responsivity spectrums measured at T = 60K are shown in Fig. 4. These two spectrums are similar in shape and peak at λ_p = 16.3 μm. The values of the cutoff wavelength λ_c and the spectral width ($\Delta\lambda$ /X) (full width at half maximum) are 17.3 μm and 20% respectively. The absolute responsivity was measured by two different methods: by comparing the detector photo-response with the photo-response of a calibrated pyroelectric detector, and by using a calibrated blackbody source. The peak responsivity Rp of the detector was 400 mA/W. Fig. 5 shows the IHET emitter and collector photo-currents versus base-collector voltage at T = 60K. The emitter was kept at - 1V bias relative to the base potential. Due to the hot electron relaxation in the wide base region, the photo-current at the collector is smaller relative to the emitter photo-current. The photo-current transfer ratio $\alpha_p = I_{C(photo)} / I_{E(photo)}$ is 1.2x10-1 at V_{CB} = -42 mV. Note that the α_d is more than three orders of magnitude smaller than α_p which clearly indicates that the dark current of IHET is four orders of magnitude smaller than the dark current of QWIP, while the photo current is reduced by an order of magnitude only. This four orders of magnitude reduction in dark current reduces the noise current by two orders of magnitude (and hence results in higher defectivity).

The optical *gain g* of the detector determined from R = (e/ hν)ηg is given by g = 0.2. The noise current[2] i_n was calculated using $i_n = \sqrt{4eI_d g\Delta f}$, where Af is the bandwidth. The calculated noise current of the detector is in = 17 pA at T = 60K. The peak D* can now be calculated from $D^* = R\sqrt{A\Delta f}/i_n$. The calculated D* between the emitter and the base (QWIP) at V_{EB} = -1V, V_{CB} = -42 mV and T = 60K is 5.8x 10^8 cm√Hz/W. The detectivity D* at the collector (IHET) is determined[15] from $D^*(IHET) = (\alpha_p/\sqrt{\alpha_d})$ D*(QWIP). Table 1 shows the QWIP and IHET defectivity D* at temperature T = 60 K for several base-collector bias voltages. The defectivity of IHET increases dramatically with decreasing temperature reaching D* = 1x10^{12} cm√Hz/W at T = 25 K and is even larger at lower temperatures.

In summary, we have demonstrated a very long wavelength (λ_c = 17.3 μm) IHET. Even though the QWIP emitters we have used were not optimized for 16 μm operation, this device clearly shows the dark current filtration capability of the energy filter. Thus, by incorporating an energy discriminating filter to a optimized QWIP18 which operate at 16 μm (D^* = 2 x 10^{10} cm√Hz/W at T = 60 K), it is possible to achieve defectivity 1 x 10^{11} cm√Hz/W at T = 60 K. This D* is adequate for most of the applications we have mentioned before. In addition, these detectors show absolutely no change in dark current and responsivity after an exposure of 6.5 Mrad of 1 MeV proton radiation [19] which is equal to 5 years of radiation damage in space. Due to excellent uniformity, radiation hardness, lower power dissipation and lower l/f noise[3] these GaAs based QWIPS and IHETs should be extremely attractive to space born applications such as EOS missions and IR astronomy.

We are grateful to K. K. Choi of the Army Research Laboratory and B. F. Levine of the AT&T Bell Laboratories for many useful discussions, and C. A. Kukkonen, V. Sarohia, S. Khanna, K. M. Koliwad, and B. A. Wilson of the Jet Propulsion Laboratory for encouragement and support of this work. The research described in this paper was performed by the Center for Space Microelectronics Technology, Jet Propulsion Laboratory, California Institute of Technology, and was jointly sponsored by the Ballistic Missile Defense Organization/Innovative Science and Technology Office, and the National Aeronautics and Space Administration, Office of Advanced Concepts and Technology.

REFERENCES

1. B. F. Levine, C. G. Bethea, G. Hasnain, J. Walker, and R. J. Malik, Appl. Phys. Lett. 53.(1988) 296.

2. B. F. Levine, J. Appl. Phys. 74, R1 (1993).

3. L. J. Kozlowski, G. M. Williams, G. J. Sullivan, C. W. Farley, R. J. Anderson, J. K. Chen, D. T. Cheung, W. E. Tennant, and R. E. DeWames, IEEE Trans. Electron Devices 38, 1124 (1991).

4. S. D. Gunapala, B. F. Levine, D. Ritter, R. A. Harem, and M. B. Panish, Appl. Phys. Lett. 58,2024 (1991).

5. S. D. Gunapala, B. F. Levine, D. Ritter, R. A. Harem, and M. B. Panish, Appl. Phys. Lett. 60,636 (1992).

6. B. K. Janousek, M. J. Daugherty, W. L. Bless, M. L. Rosenbluth, M. J. O'Loughlin, H. Kanter, F. J. De Luccia, and L.. E. Perry, J. Appl. Phys. 67,7608 (1990).

7. S. R. Andrews and B. A. Miller, J. Appl. Phys. 70,993 (1991).

8. K. K. Choi, M. Dutta, P. G. Newman, M. L. Saunders, and G, L. Iafrate, Appl. Phys. Lett. 57, 1348 (1990).

9. L. S. *Yu* and S. S. Li, Appl. Phys. Lett. 59, 1332 (1991).

10. A. G. Steele, H. C. Liu, M. Buchanan, and Z. R. Wasilewski, Appl. Phys. Lett. 59, 3625 (1991).

11. S. D. Gunapala, B. F. Levine, L. Pfeiffer, and K. West, J. Appl. Phys. 69, 6517 (1990).

12. M. J. Kane S. Millidge, M. T. Emeny, D. Lee, D. R. P. Guy, and C. R. Whitehouse in Ref. 2.

13. C. S. Wu, C. P. Wen, R. N. Sate, M. Hu, C. W. Tu, J. Zhang, L. D. Flesner, L. Pham, and P. S. Nayer, IEEE Tran. Electron Devices 39,234 (1992).

14. K. K. Choi, M. Dutta, and R. P. Moerkirk, Appl. Phys. Lett. 58, 1533 (1991).

15. K. K. Choi, M. Taysing-Lara, L. Fotiadis, and W. Chang, Appl. Phys. Lett. 59, 1614 (1991).

16. K. K. Choi, L. Fotiadis, M. Taysing-Lara, and W. Chang, Appl. Phys. Lett. 59, 3303 (1991).

17. B. F. Levine, C. G. Bethea, G. Hasnain, V. O. Shen, E. Pelve, R. R. Abbott, and S. J. Hsieh, Appl. Phys. Lett. 56,851 (1990).

18. G. Sarusi, B. F. Levine, S. J. Pearton, K. M. S. V. Bandara, and R. E. Leibenguth (to be published).
19. S. D. Gunapala, J. S. Park, T. L. Lin, and J. K. Liu (to be published).

TABLE I. Comparison of QWIP and IHET defectivity D* at temperature T = 60 K for several base-collector bias voltages.

V_{BC} (mV)	$\alpha_p / \sqrt{\alpha_d}$	D* QWIP (cm√Hz/W)	D* IHET (cm√Hz/W)
-30	0.72	6.0X10 ^{8}	4.3X1 08
-35	1.17	5.9X10 ^{8}	6.9x1 O ^{8}
-40	3.98	5.9X10 ^{8}	2.3x1 O ^{9}
-42	14.14	5.8x10 ^{8}	8.2x10 ^{9}

FIGURE CAPTIONS

FIG. 1 Theoretical and experimental (solid) dark current-voltage curves at T = 60K. Dotted curve shows the dark current (theoretical) due to thermionic emission only. Dashed curve shows the total dark current (thermionic + tunneling + thermionic assisted) versus bias voltage.

FIG.2 Conduction-band diagram of a infrared hot electron transistor, which utilizes bound to continuum intersubband transition. The inset shows the schematic diagram of IHET.

FIG.3 IHET emitter and collector dark currents versus base-collector voltage at T = 60K. Emitter bias was kept at -1 V relative to the base potential. This figure also shows the lower energy dark current filtration capability of the quantum filter.

FIG.4 Emitter and collector responsivity spectra at temperature T = 60K. Emitter was kept at -IV bias relative to the base and collector.

FIG.5 IHET emitter and collector photo-currents versus base-collector voltage at T = 60K. Emitter was kept at - IV bias relative to the base potential.

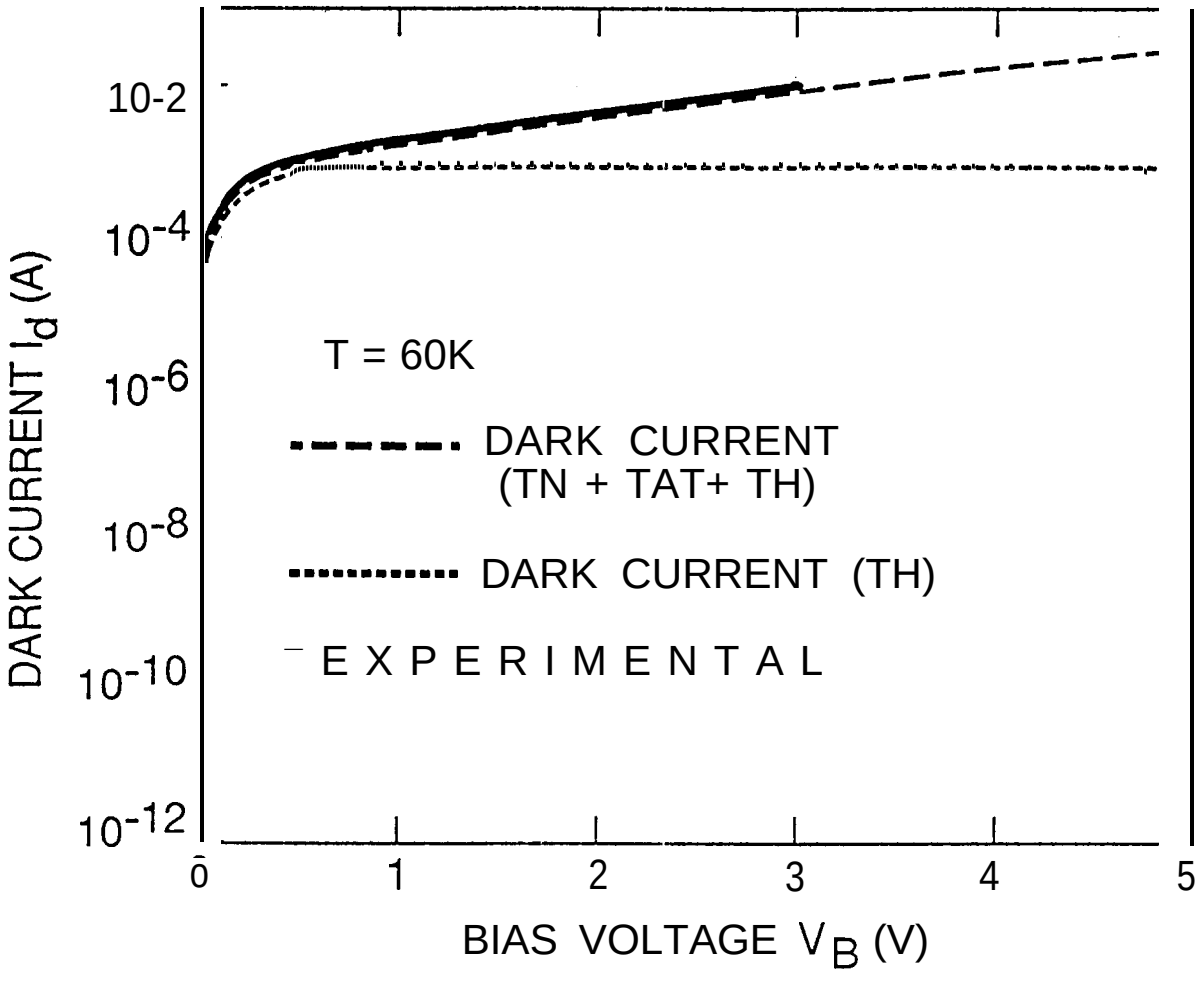
10-2
10-4
10-6
10-8
10-10
10-12
DARK CURRENT I_d (A)
T = 60K
DARK CURRENT
(TN + TAT+ TH)
DARK CURRENT (TH)
EXPERIMENTAL
0
1
2
3
4
5
BIAS VOLTAGE V_B (V)

FIG. 1

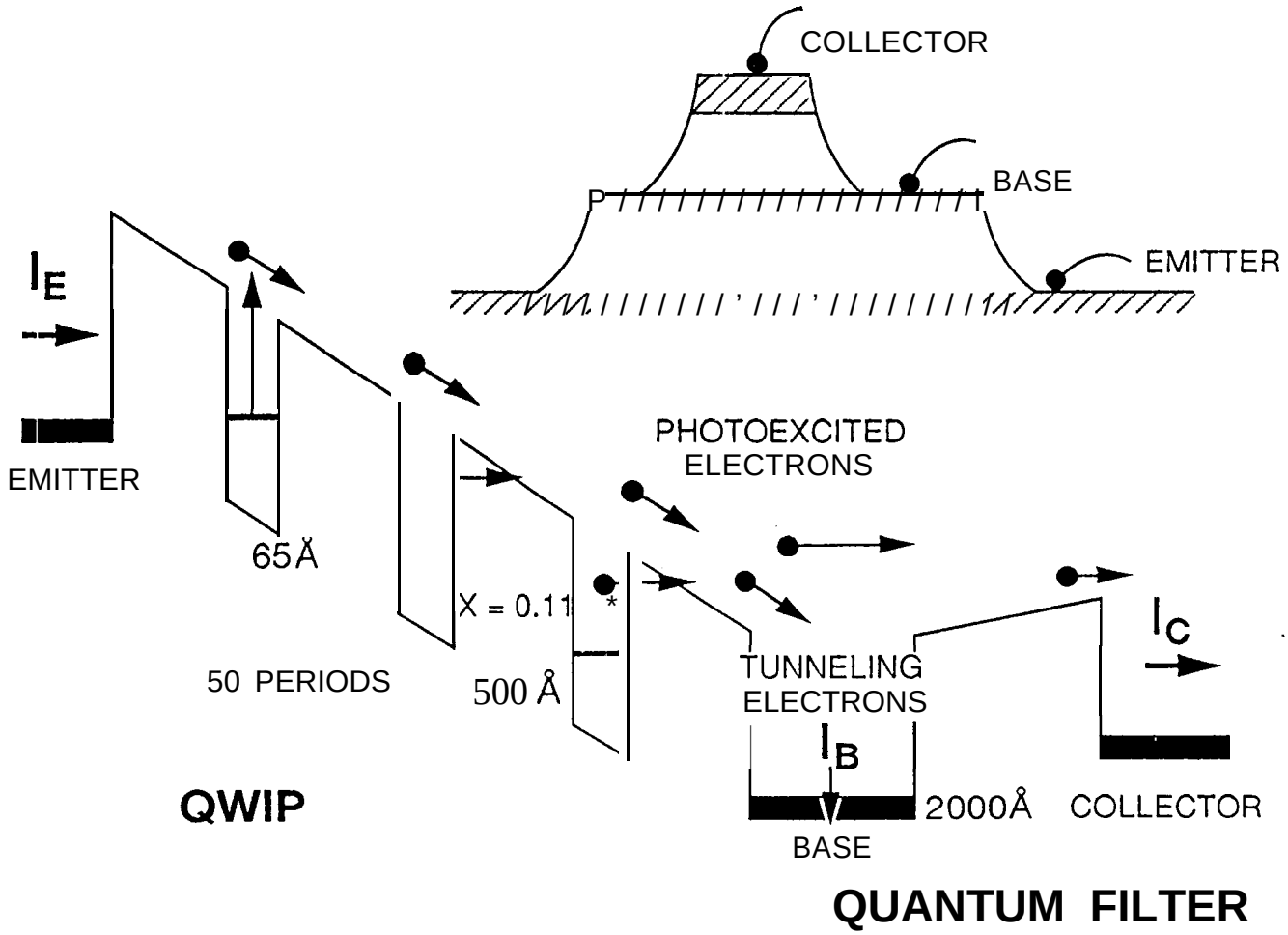
COLLECTOR
BASE
P
EMITTER
I_E
EMITTER
65Å
50 PERIODS
X = 0.11
500 Å
PHOTOEXCITED
ELECTRONS
TUNNELING
ELECTRONS
I_B
I_C
2000Å
COLLECTOR
BASE
QWIP
QUANTUM FILTER

FIG.

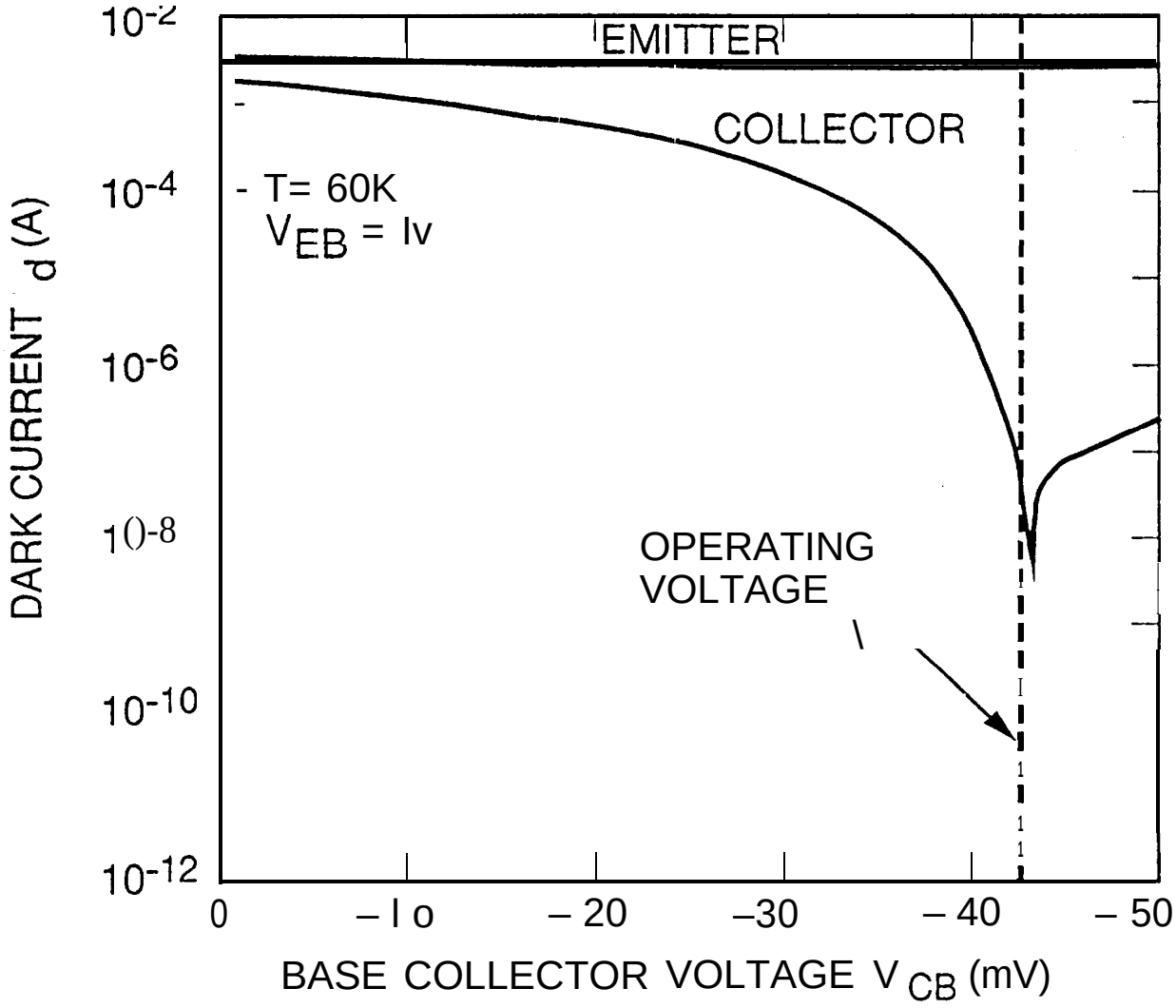
EMITTER
COLLECTOR
- T= 60K
V_{EB} = Iv
OPERATING
VOLTAGE
DARK CURRENT $_d$ (A)
10^{-2}
10^{-4}
10^{-6}
10-8
10^{-10}
10^{-12}
0
– I o
– 20
–30
– 40
– 50
BASE COLLECTOR VOLTAGE V_{CB} (mV)

FIG.

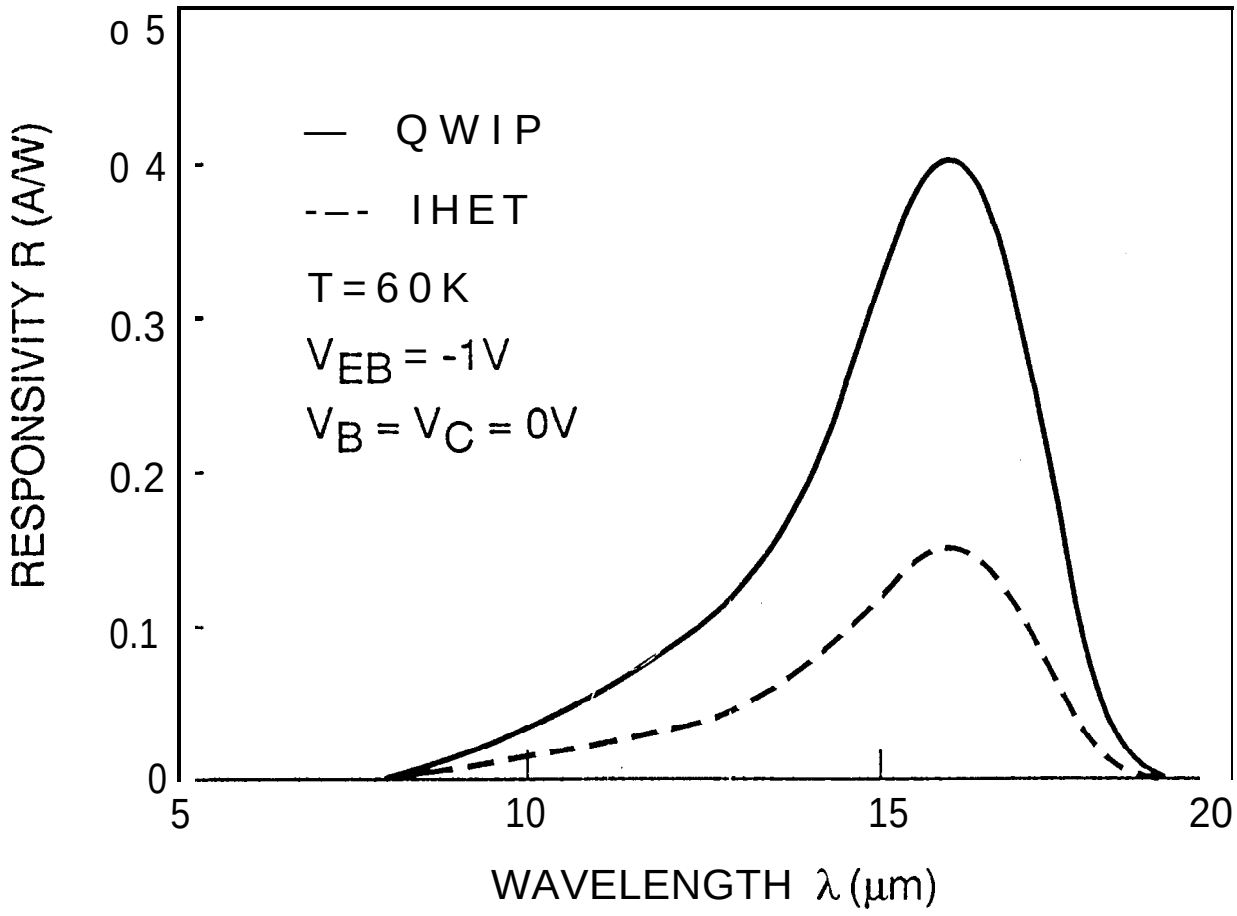
o 5
0 4
0.3
0.2
0.1
0
RESPONSIVITY R (A/W)
— QWIP
--- IHET
T = 60 K
V_{EB} = -1V
$V_B = V_C$ = 0V
5
10
15
20
WAVELENGTH λ (μm)

FIG.

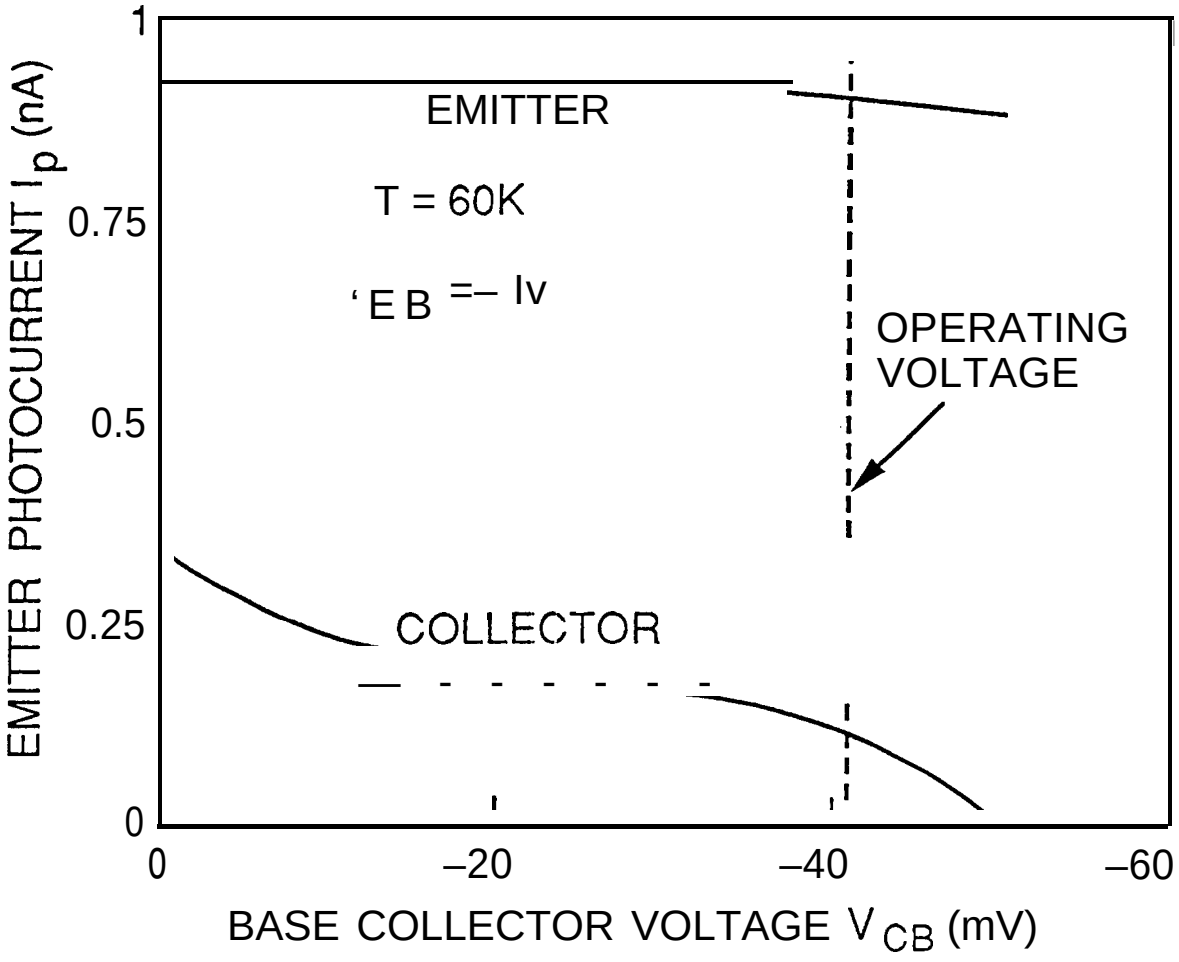
1
0.75
0.5
0.25
0
EMITTER PHOTOCURRENT I_p (nA)
EMITTER
T = 60K
$I_{EB} = -I_V$
OPERATING VOLTAGE
COLLECTOR
0
–20
–40
–60
BASE COLLECTOR VOLTAGE V_{CB} (mV)

FIG.